Seasonal shift in airborne microbial communities

Romie Tignat-Perrier, Aurélien Dommergue, Alban Thollot, Olivier Magand, Pierre Amato, Muriel Joly, Karine Sellegri, Timothy M. Vogel, Catherine Larose

Seasonal shift in airborne microbial communities linked to land use

Romie Tignat-Perrier[1,2*], Aurélien Dommergue[1], Alban Thollot[1], Olivier Magand[1], Pierre Amato[3], Muriel Joly[3], Karine Sellegri[3], Timothy M. Vogel[2], Catherine Larose[2]

[1]Institut des Géosciences de l'Environnement, Université Grenoble Alpes, CNRS, IRD, Grenoble INP, Grenoble, France

[2]Environmental Microbial Genomics, CNRS UMR 5005 Laboratoire Ampère, École Centrale de Lyon, Université de Lyon, Écully, France

[3]Institut de Chimie de Clermont-Ferrand, CNRS UMR 6096 Université Clermont Auvergne-Sigma, Clermont-Ferrand, France

*romie.tignat@univ-grenoble-alpes.fr

Highlights

-Airborne microbial communities showed a seasonal shift at the puy de Dôme elevated site

-Dominant microbial taxa showed different trends throughout the year

-Summer results in higher concentrations of plant-associated microbes in the air

-Winter results in higher concentrations of soil and dead material-associated microbes

-Seasonal changes in the underlying ecosystems likely drive microbial seasonal shift

Abstract

Microorganisms are ubiquitous in the atmosphere. Global investigations on the geographical and temporal distribution of airborne microbial communities are critical for identifying the sources and the factors shaping airborne communities. At mid-latitude sites, a seasonal shift in both the concentration and diversity of airborne microbial communities has been systematically observed in the planetary boundary layer. While the factors suspected of affecting this seasonal change were hypothesized (*e.g.*, changes in the surface conditions, meteorological parameters and global air circulation), our understanding on how these factors influence the temporal variation of airborne microbial communities, especially at the microbial taxon level, remains limited. Here, we investigated the distribution of both airborne bacterial and fungal communities on a weekly basis over more than one year at the mid-latitude and continental site of puy de Dôme (France; +1465 m altitude above sea level). The seasonal shift in microbial community structure was likely correlated to the seasonal changes in the characteristics of puy de Dôme's landscape (croplands and natural vegetation). The airborne microbial taxa that were the most affected by seasonal changes trended differently throughout the seasons in relation with their trophic mode. In addition, the windy and variable local meteorological conditions found at puy de Dôme were likely responsible for the intraseasonal variability observed in the composition of airborne microbial communities.

Keywords: atmospheric microorganisms, bioaerosols, planetary boundary layer, amplicon sequencing, biosphere-atmosphere interactions

Introduction

Thousands to millions of diverse microbial cells per cubic meter of air are transported among aerosols with their diversity shown to depend on geographic location[1] and time of year[2]. These microorganisms might be active, since some airborne microbial isolates were shown in

laboratory studies to sustain metabolic activity using organic acids found in the atmosphere[3–5]. Understanding the global distribution of airborne microbial communities is critical for determining how airborne microorganisms might influence atmospheric chemistry[4], meteorological processes such as cloud and precipitation formation[6], as well as human and crop health[7]. Recent large geographical and spatial investigations highlighted the major contribution of the local landscapes and local environmental factors in the observed distribution of airborne microbial communities in the planetary boundary layer[1,8]. The composition of airborne microbial communities is closely related to the nature of the surrounding landscapes (ocean, agricultural soil, forest *etc*.) from which local meteorology (especially wind direction and speed) controls microbial cell emission rates[1]. Studies on airborne microbial communities at mid-latitude sites (aerosol-, cloud water- and precipitation-associated microorganisms) reported seasonal changes in both microbial biomass and biodiversity[2,9–13]. The seasonal variability was associated to changes in surface conditions[10,11], meteorological conditions[2,9] and/or changes in the global air circulation[9,13]. Yet, our understanding on how these potential factors impact airborne microbial community composition, and more specifically the microbial taxa individually, remains limited. Here, we investigated the distribution of airborne microbial communities and specific microbial taxa at the mid-latitude and continental site of puy de Dôme (France; +1465 m altitude above sea level). We monitored the diversity and abundance of bacterial and fungal communities in the troposphere on a weekly basis for more than a year (June 2016 to August 2017). These microbial community metrics were evaluated in relation to the local meteorology and particulate matter chemical composition, and puy de Dôme local landscape was evaluated based on the MODIS satellite images. While a number of studies focusing on microorganisms in clouds has been carried out at puy de Dôme[3,4,14–17], no investigation was conducted in the dry troposphere and at such a high temporal resolution. Puy de Dôme is surrounded mainly by

croplands and vegetation (*i.e.* > 80% of the surrounding landscapes in a perimeter of 50 km) whose surface characteristics change drastically over the four different seasons (summer, autumn, winter and spring). These seasonal changes in landscape were related to the temporal variability of airborne microbial community composition at the microbial taxon level.

Material and Methods

Sites and Sampling

A size selective high volume air sampler installed at the puy de Dôme (PDD) meteorological station terrace was used to collect particulate matter on quartz fiber filters every week from June 2016 to August 2017 (**Table S1**). The sampler was equipped with a PM10 size-selective inlet in order to collect particulate matter smaller than 10 µm (PM10) and sampling was done as presented in Dommergue et al. (2019)[18]. Overall, the dataset was composed of fifty-three samples with an average normalized collected volume of 9100 m^3 (**Table S1**). Quartz fiber filters were heated to 500°C for 8 hours to remove traces of organic carbon including DNA. All the material including the filter holders, aluminium foils and plastic bags in which the filters were transported were sterilized using UV radiation as detailed in Dommergue et al., (2019)[18]. A series of field and transportation blank filters were carried out to monitor the quality of the sampling protocol as presented in Dommergue et al. (2019)[18]. PDD is a mid-altitude (+ 1465 m) site surrounded by croplands, an urban area (Clermont-Ferrand) and forests within a 50 km perimeter (**Fig. 1**). Monthly NASA satellite images of puy de Dôme surrounding surfaces (https://wvs.earthdata.nasa.gov/) are shown in **Fig. S1**. The Atlantic coast and Mediterranean Sea are at around 320 km and 240 km from PDD, respectively.

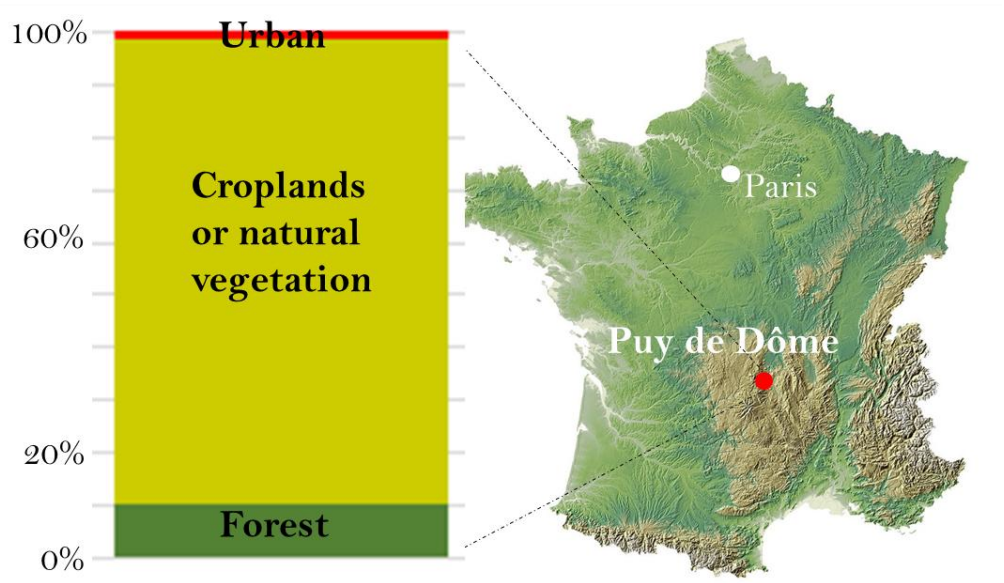

Fig. 1. Geographical location and landscape of the sampling site. Map showing the location of the puy de Dôme mountain in France and relative surfaces types surrounding the site in a perimeter of 50 km based on the MODIS satellite images. Cropland and vegetation areas comprise > 80% of the surrounding landscapes, while forest and urban areas (mainly Clermont-Ferrand) comprise < 20% of the surrounding landscapes.

DNA extraction

We extracted DNA from 3 punches (diameter of one punch: 38 mm) from the quartz fiber filters using the DNeasy PowerWater kit with some modifications as detailed in Dommergue et al. (2019)[18]. During cell lysis, an one hour heating step at 65°C followed by a 10-min vortex treatment at maximum speed and a centrifugation using a syringe to separate the filter debris from the lysate were added to the DNeasy PowerWater DNA extraction protocol[18]. DNA concentration was measured using the High Sensitive Qubit Fluorometric Quantification (Thermo Fisher Scientific) then stored at -20°C.

Real-Time qPCR analyses

The bacterial cell concentration was approximated by the number of 16S rRNA gene copies per cubic meter of air and the fungal cell concentration was approximated by the number of 18S rRNA gene copies per cubic meter of air. Primers and methodology are presented in Tignat-Perrier et al. (2019)[1].

MiSeq Illumina amplicon sequencing

16S rRNA gene sequencing: library preparation, reads quality filtering and taxonomic annotation. The V3-V4 region of the 16S rRNA gene was amplified and libraries were prepared as presented in Tignat-Perrier et al. (2019)[1]. The amplicons were sequenced by paired-end MiSeq sequencing using the V3 Illumina technology with 2 x 250 cycles. Reads were filtered based on quality using FASTX-Toolkit (http://hannonlab.cshl.edu/fastx_toolkit/), assembled using PANDAseq[19], and annotated using RDP Classifier[20] and the RDP 16srRNA database as detailed in Tignat-Perrier et al. (2019)[1]. RDP classifier was used in part to avoid errors due to sequence clustering. The number of sequences per sample and the percentage of sequences annotated at the genus level were evaluated using a home-made R script. The sequences annotated as chloroplasts by RDP were manually removed.

ITS rRNA gene sequencing: library preparation, reads quality filtering and taxonomic annotation. The ITS2 region of the ITS was amplified libraries were prepared as presented in Tignat-Perrier et al. (2019)[1]. The amplicons were sequenced by a paired-end MiSeq sequencing using the technology V2 of Illumina with 2 x 250 cycles. Reads were filtered based on quality using FASTX-Toolkit, assembled using PANDAseq, and annotated at the species level[21] using RDP Classifier and the RDP fungallsu database as detailed in Tignat-Perrier et al. (2019)[1]. The number of sequences per sample and the percentage of sequences annotated at the species level were evaluated using a home-made R script.

144 The number of reads per sample and per sequencing (V3-V4 regions of the 16S rRNA gene
145 and the ITS2 region of the ITS) is presented in the **Table S1**. Samples with less than 6000
146 reads were removed. Samples from the same season were pooled and rarefaction curves per
147 season were done (**Fig. S2**).
148
149 *Estimation of the trophic mode of the fungal species*
150 We used the FUNGuild software[22] to assign the trophic mode of the fungal species (RDP
151 classifier based annotation). Fungal species annotated to a trophic mode with the level
152 confidence "Possible" were grouped in the "not classified" fungi. Then, we calculated the
153 percentage represented by each trophic mode per sample. Heatmaps were done using the R
154 package gplots.
155
156 *Chemical analyses*
157 The elemental carbon (EC), organic carbon (OC), sugar anhydrides and alcohols
158 (levoglucosan, mannosan, galactosan, inositol, glycerol, erythriol, xylitol, arabitol, sorbitol,
159 mannitol, trehalose, rhamnose, glucose, fructose and sucrose), soluble anions (MSA, SO_4^{2-},
160 NO_3^-, Cl^-, Ox) and cations (Na^+, NH_4^+, K^+, Mg^{2+}, Ca^{2+}) concentrations were analyzed as
161 presented in Dommergue et al. (2019)[18].
162
163 *Meteorological data*
164 Meteorological parameters such as wind speed and direction, temperature, relative humidity
165 and UV were collected (Vaisala instrument). For each sample, the backtrajectories of the air
166 masses were calculated over 3 days before the sampling using HYSPLIT[23] (maximum height
167 above ground level: 1 km).
168

Graphical and Statistical analyses

Environmental variables. For chemical species, air concentrations in ng per cubic meter of air were used in the analyses. The chemical table was log10-transformed to approach a Gaussian distribution (verified on a Q-Q plot and tested using the Shapiro-Wilk test), and a hierarchical cluster analysis (average method) was done on the Euclidean distance matrix using the vegan and ade4 R packages. Meteorological data were used to do the wind roses using the openair R package[24]. Backtrajectories of the air masses over three days were plotted on maps using the openair R package, and the relative surfaces of the landscapes (MODIS land surfaces) air masses over flown were calculated.

Diversity statistics and Multivariate analyses. Before doing the multivariate analyses, the raw abundances of the taxa (bacterial genera and fungal species) were transformed into relative abundances to counter the heterogeneity in the number of sequences per sample. A hierarchical cluster analysis (average metric) on the Bray-Curtis dissimilarity matrix was done using the vegan and ade4 R packages[25]. We have defined the seasons as following: we adjusted the beginning and ending administrative dates of the seasons (*i.e.* summer: 20th of June to 22th of September; autumn: 23th of September to 21th of December; winter: 22th of December to 19th of March; spring: 20th of March to 19th of June) based on the weekly mean temperature (**Fig. S3**). France goes through a cycle of four strong seasons characterized by distinctive weather: the summer is characterized by higher temperatures, a longer daylight period and the period of fructification of fruiting plants; the autumn is the harvest period of most annual crops and a preparation period for dormancy; winter is characterized by the lowest temperatures, frequent precipitation (rain and snow) and high air humidity; and finally the spring is characterized by milder weather, snow melting, budding and flowering. To access the variability of microbial population structure within the seasons, we averaged the degrees of dissimilarity obtained from the Bray-Curtis matrix for each pair of samples from

194 the same season, subtracted these values from 1 to get similarity values and divided the
195 similarity values by the standard deviation (as detailed in Tignat-Perrier et al., 2019[1]).
196 Spearman correlations were calculated to test the correlation between microbial abundance
197 and richness and quantitative environmental factors using the Hmisc R package[26]. ANOVA
198 analyses were used to test the influence of qualitative factors such as season and year on both
199 bacterial and fungal abundance and richness using the vegan R package, followed by
200 TukeyHSD tests to identify which group revealed a significantly different mean. A distance-
201 based redundancy analysis (RDA – linear or non-linear correlation) was carried out to
202 evaluate the part of the variance between the samples explained by the seasons, chemistry
203 and/or meteorology, and an ANOVA was carried out to test each variable using the vegan and
204 ade4 R packages. Venn diagrams using the R package VennDiagram were done to access the
205 shared and unique bacterial genera and fungal species from each season after rarefaction on
206 the raw abundances (rarefaction at the minimum number of reads). A Mantel test between the
207 Bray-Curtis matrices based on the bacterial genera and fungal species was used to evaluate
208 similarities in the distribution of the samples. A Mantel test was done between the Bray-Curtis
209 matrix based on either the bacterial or the fungal diversity and the Euclidean distance matrix
210 based on the chemical variables or meteorology to evaluate the similarities in the distribution
211 of the samples.
212
213
214 Results
215 ***Temporal distribution of airborne microbial communities***
216 *Airborne microbial abundance.* Airborne bacterial and fungal concentrations (estimated by
217 the number of 16S rRNA and 18S rRNA gene copies) were positively correlated (r=0.77,
218 pvalue=7.9×10^{-11}) and varied between 1.8×10^{3} and 2.1×10^{7} cells per cubic meter of air and 3

and 1.0×10^5 cells per cubic meter of air, respectively. Neither bacteria nor fungal abundance significantly varied with season (pvalues=0.20 and 0.38, respectively), but the highest concentrations observed occurred in spring and summer for both bacteria and fungi (**Table 1** and **Fig. S4**).

Table 1. Microbial concentration and richness estimations depending on the season. Concentrations of bacterial and fungal ribosomal gene copies and associated richness (number of bacterial genera and fungal species) averaged for each season and relative standard deviation. Reference letters indicate the group membership based on Tukey's HSD post hoc tests (done only for the estimated bacterial richness as the ANOVA showed differences between the groups).

Season	Average bacterial concentration (number of 16S rRNA gene copies/m^3 of air)	Average fungal concentration (number of 18S rRNA gene copies/m^3 of air)	Average Chao1 bacterial richness estimation (estimated number of bacterial genera)	Average Chao1 fungal richness estimation (estimated number of fungal species)
PDD spring	2.7×10^{6} +/- 6.2×10^{6}	4.6×10^{3} +/- 1.1×10^{4}	4.8×10^{2} +/- 1.4×10^{2} ^{ab}	4.7×10^{2} +/- 9.3×10^{1}
PDD summer	8.5×10^{5} +/- 1.3×10^{6}	1.6×10^{4} +/- 2.8×10^{4}	6.1×10^{2} +/- 1.5×10^{2} ^{a}	4.6×10^{2} +/- 1.9×10^{2}
PDD autumn	2.2×10^{5} +/- 4.0×10^{5}	3.2×10^{3} +/- 4.6×10^{3}	4.3×10^{2} +/- 1.2×10^{2} ^{b}	3.6×10^{2} +/- 1.9×10^{2}
PDD winter	3.6×10^{5} +/- 9.0×10^{5}	7.4×10^{2} +/- 9.4×10^{2}	3.9×10^{2} +/- 1.4×10^{2} ^{b}	3.0×10^{2} +/- 1.8×10^{2}

Airborne microbial richness. The observed richness varied between 150 and 674 genera of bacteria, and 84 and 649 species of fungi. The estimated richness (Chao1) varied between 234 and 897 bacterial genera and 97 and 820 fungal species. The estimated bacterial richness was higher in summer compared to winter and autumn (pvalue=4.5×10^{-4}; **Table 1**). The estimated fungal richness also was highest in summer, while not significant due to relatively higher

variability (pvalue=0.18; **Table 1**). A rough correlation was found between the estimated richness estimations and concentration estimations for both bacteria and fungi (r=0.41, pvalue=3.0×10^{-3} and r=0.50, pvalue=4.6×10^{-4}, respectively).

Consistently with highest richness, summer had the highest percentage of unique bacterial genera (16% or 198/1239 of the genera in summer were only present in this season), followed by autumn (4.5% or 39/873), spring (4.4% or 42/953) and winter (4.3% or 37/864) (**Fig. S5**). This was also observed for unique fungal species with the highest percentage observed in summer (28.4% or 457/1606), followed by autumn (17.4% or 191/1097), spring (14.4% or 172/1196) and winter (8% or 63/786) (**Fig. S5**). The majority of the bacterial genera and fungal species observed was present throughout the year, (*i.e.* they were shared by all the seasons; **Fig. S5**).

The five most abundant bacterial genera were *Bacillus* (15.6% in average) (Firmicutes), *Hymenobacter* (9.2%) (Bacteroidetes), *Sphingomonas* (7.4%) (Alphaproteobacteria), *Methylobacterium* (5.1%) (Alphaproteobacteria) and *Thermoactinomyces* (4.6%) (Firmicutes). Their relative abundance varied over the year: *Bacillus* was abundant throughout the year and dominated the community from summer to spring, while *Hymenobacter* increased in autumn and winter (19.2% and 13.9% respectively). The twenty-five most abundant bacterial genera and fungal species observed in each season are listed in **Table S2**. In fungi, the five most abundant species were *Pseudotaeniolina globosa* (11.5% in average), *Cladophialophora proteae* (7.9%), *Alternaria* sp. BMP_2012 (4%), *Cladophialophora minutissima* (4%) and *Naevala minutissima* (3.1%). Similar to bacteria, their relative abundance varied seasonally: *Cladophialophora proteae* represented 13.3% of the community in winter and only 0.3% in summer, when *Alternaria* dominated (10.8%); autumn was dominated by *Pseudotaeniolina globosa* and *Cladophialophora proteae* (16.4% and 15.6%,

respectively), while *Naevala minutissima* was detected only in spring and summer, dominating in spring (10.1%).

Airborne microbial structure. The hierarchical cluster analyses of the samples based on both the bacterial (genus level) and fungal (species level) community structures are shown in **Fig. 2**; these were highly similar (r=0.50 and pvalue<0.001). The samples tended to group by season (anosim r=0.30 and r=0.49 with pvalues=0.001 for bacterial and for fungal communities, respectively; **Fig. 2**) with season explaining 17% and 22% of the variability in the community structures, respectively (pvalues=0.001). The distribution of the summer samples based on fungal species was different between 2016 and 2017 (pvalue=0.001). The intraseasonal variability in community structure was greatest in spring and smallest in summer for bacteria and conversely greatest in autumn and smallest in winter for fungi (**Table S3**). The relative abundances of fungal saprotrophs and symbiotrophs (like *Balospora myosura*, *Strobilurus albipilatus*, *Pseudotaeniolina globosa*) (**Fig. 3**) were greater in autumn and winter than during the rest of the year (pvalue=4.3×10^{-5} and 0.5 for saprotrophs and symbiotrophs, respectively). The relative abundance of fungal pathotrophs was greater in the spring and summer periods (pvalue=0.51 – **Fig. 3**). Examples of phytopathogens increasing in relative abundance during the summer and/or spring are *Mycosphaerella graminicola* (wheat plant pathogen – **Fig. S6**), *Microdochium majus* (cereal pathogen – **Fig. S6**), *Blumeria graminis* (powdery mildew pathogen – **Fig. S6**), *Ustilago hordei* (maize pathogen – **Fig. S6**), *Botryotinia fuckeliana* (gray mold disease) and *Erysiphe alphitoides* (powdery mildew on oak trees). However, the number of fungal species associated to pathogenic and saprophytic trophic modes was greatest in spring and summer, whereas symbiotrophs were mostly found in summer and autumn (**Table S4**).

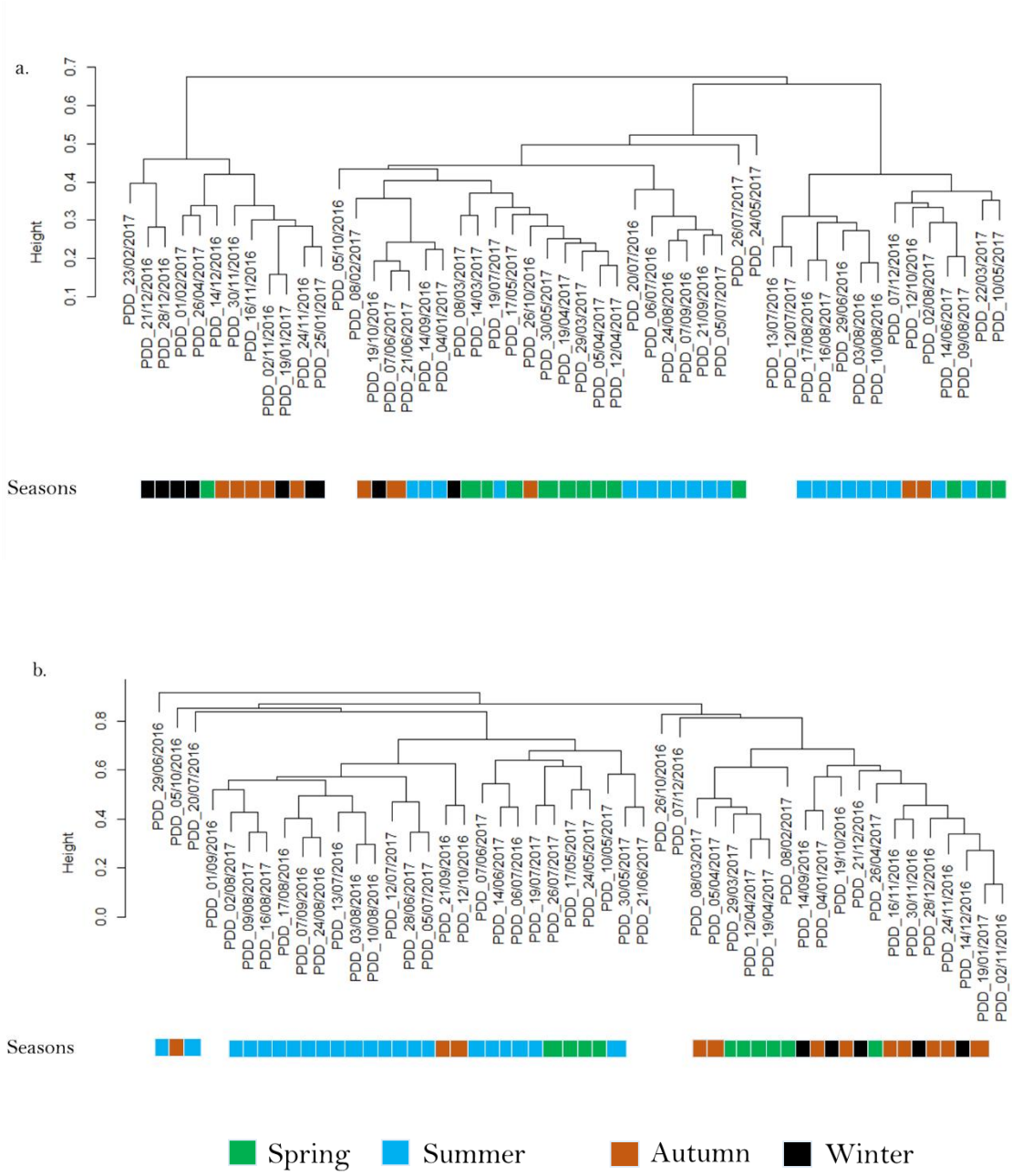

Fig. 2. Distribution of the samples based on the microbial community structure. Hierarchical cluster analysis (average method) of airborne community structures of bacteria (16S rRNA gene – a.) and fungi (ITS region – b.) based on Bray-Curtis dissimilarity matrices. The season corresponding to each sample is indicated as a frieze (black=winter, blue=summer, green=spring and brown=autumn) that has been split into three based on the three major clusters observed on the hierarchical cluster analyses.

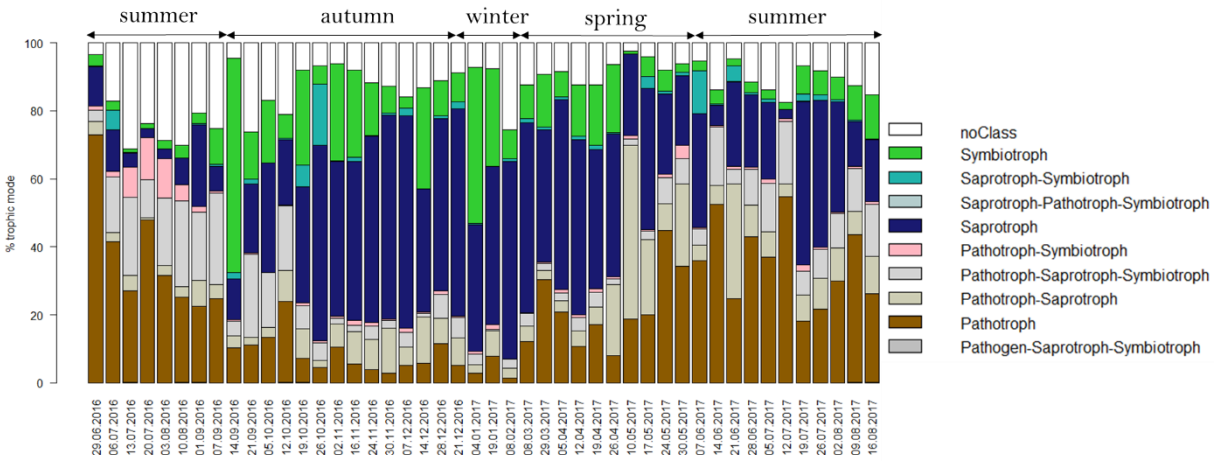

Fig. 3. Distribution of the trophic modes of the fungal species identified. Each fungal species detected was associated to either a specific trophic mode, different trophic modes or no trophic mode (« noClass ») using the FUNGuild software, then the proportions of species belonging to each trophic mode were summed.

When looking at the fifty most abundant bacterial genera and fungal species of the dataset that mainly controlled the distribution of the samples based on the microbial community structure (they represented 79.6% or 881898 sequences/1107323 and 71.8% or 367440 sequences/511738 of all the bacterial and fungal sequences, respectively), we observed three different patterns in the temporal variation of their relative abundance (**Fig. 4** and **5**). The period during which the relative abundance increased varied in length and depended on the microorganism. First, some taxa were mostly abundant during the cold period of the year: 20% (10/50) of the bacterial genera and 34% (17/50) of the fungal species showed a higher relative abundance in winter and/or autumn compared to the other seasons. This was the case with *Hymenobacter* and *Pseudotaeniolina proteae* for example, whose relative abundances suddenly increased between November 2016 and February 2017, and between October 2016 and April 2017, respectively (**Fig. 4a**). Fungal taxa belonging to this group were almost

exclusively saprotroph and/or pathotroph (**Table S5**). Second, some taxa were mostly abundant during summer and/or spring: 42% (21/50) of the bacterial genera and 46% (23/50) of the fungal species. For example, *Sphingomonas* and *Alternaria* sp. BMP_2012 relative abundances started to decrease in late summer/early autumn and increased again in the late spring (**Fig. 4b**). Fungal taxa belonging to this group were pathotroph, symbiotroph or saprotroph (**Table S5**). Finally, some taxa had no clear pattern in their relative abundance (*i.e.* stable or randomly variable over the year): 38% (19/50) of the bacterial genera and 20% (10/50) of the fungal species (e.g., *Bacillus* and *Phaeosphaeria herpotrichoides*) (**Fig. 4c**). Fungal taxa belonging to this group were mostly saprotroph (**Table S5**).

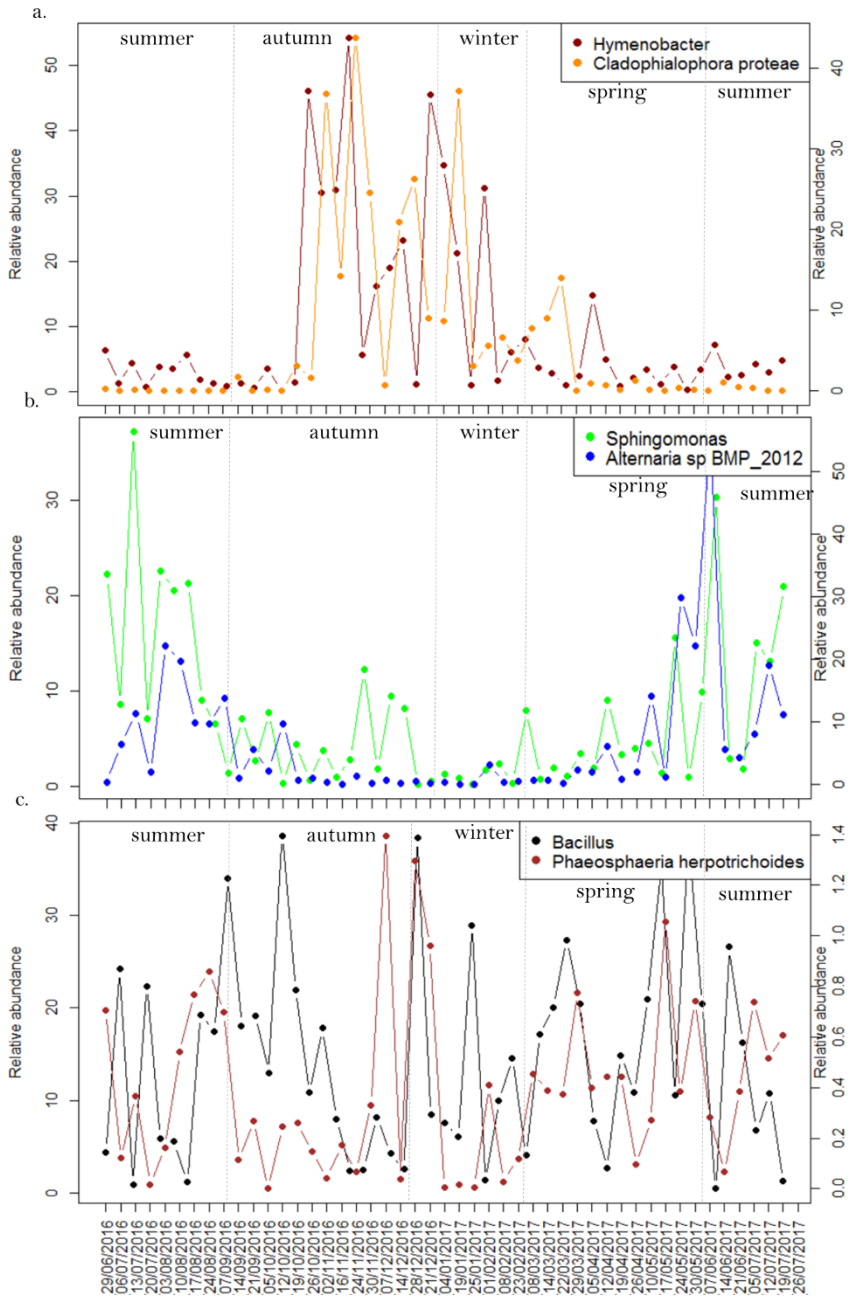

Fig. 4. Temporal evolution of the relative abundance of several fungal species and bacterial genera among the airborne communities over the year.

a) Higher relative abundance in autumn and winter: examples of the fungal species *Cladophialophora proteae* (right y scale) and the bacterial genus *Hymenobacter* (left y scale);

b) Higher relative abundance in spring and summer: examples of the fungal species *Alternaria* sp. BMP 2012 (right y scale) and the bacterial genus *Sphingomonas* (left y scale);

c) No trend of the relative abundance over the year: examples of the fungal species *Phaeosphaeria herpotrichoides* (right y scale) and the bacterial genus *Bacillus* (left y scale).

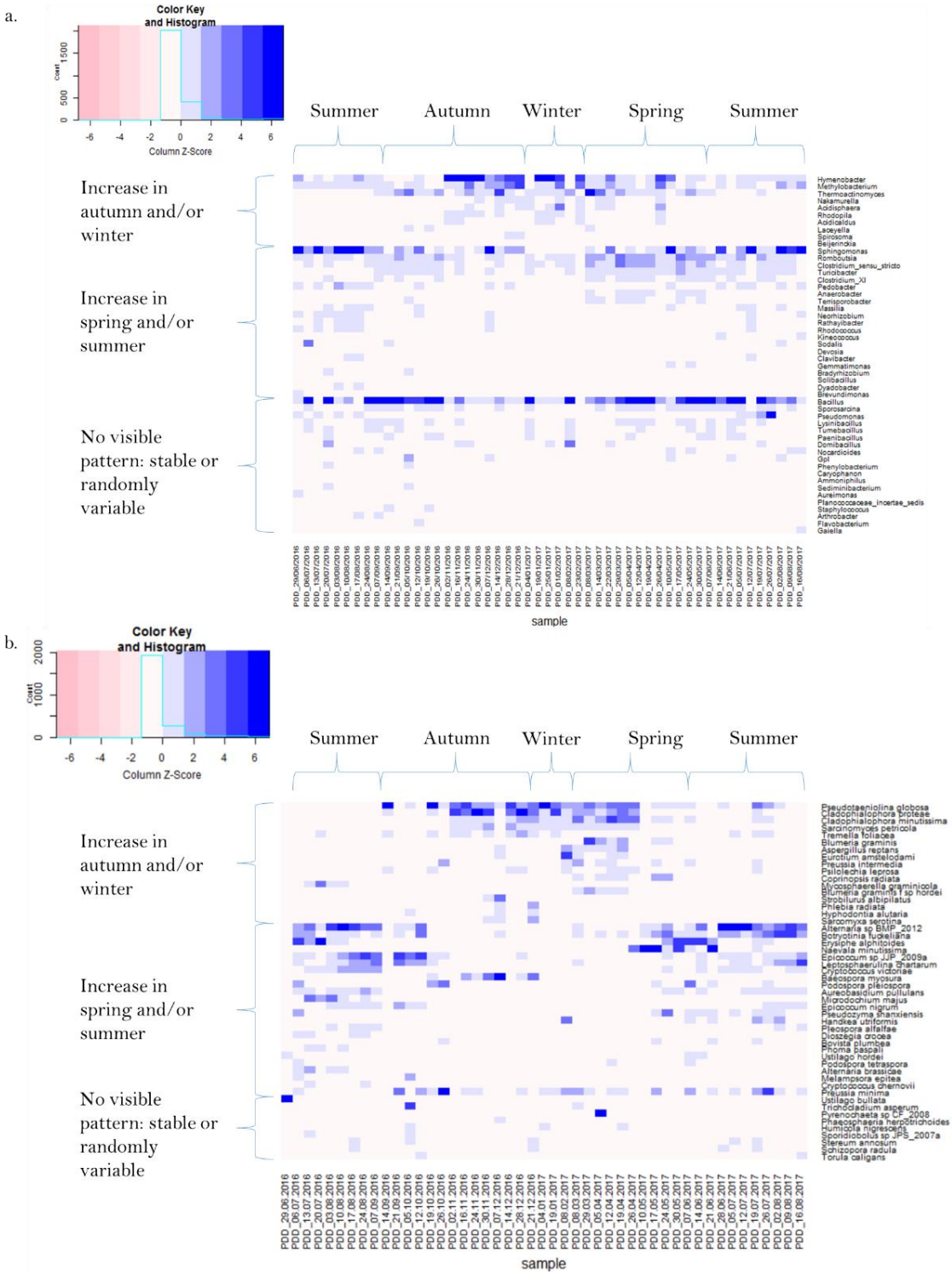

Fig. 5. Temporal evolution of the relative abundances of the dominant microbial taxa. Heatmaps showing the temporal evolution of the relative abundances (centered and scaled) of the fifty most abundant bacterial genera (a.) and fungal species (b.) in the dataset. The microbial taxa are grouped based on the three general trends exemplified in **Fig. 4**.

344

345

346 ***Atmospheric PM10 chemistry***

347 The hierarchical cluster analysis of the samples based on the PM10 chemical profile is shown
348 in **Fig. S7**. Chemical concentrations varied significantly with season (pvalues<0.05) for all the
349 compounds measured except Cl^-, NO_3^-, NH_4^+ and rhamnose (pvalues>0.05) (**Table S6**).
350 Seasons explained 38% of the variance in the distribution of the samples based on the
351 chemical composition (pvalue=0.001). When looking at the weekly variation of the
352 concentrations of the different compounds, we observed general trends of seasonal variations
353 (as observed for microbial communities). Some increased during autumn/winter compared to
354 spring/summer (galactosan, levoglucosan and mannosan), while some others decreased
355 (erythriol, glucose, trehalose, sorbitol, xylitol, inositol, SO_4^{2-}, OC, MSA) (**Fig. S8**). The
356 sample distribution based on bacterial and fungal community structures were correlated to
357 their distribution based on the overall PM10 chemistry (Mantel test r=0.25 pvalue=0.001 and
358 0.41 pvalue=0.001, respectively) (see RDA analyses in **Fig. S9**). Specific chemical
359 compounds were the main contributors to these correlations (*i.e.* the polyols, MSA and Na^+
360 for the fungal communities, and organic carbon, Na^+, Cl^- and erythriol for the bacterial
361 communities). Consistent with seasonal patterns observed for both microbial community
362 structures and chemical composition, we observed strong positive and negative correlations
363 between the concentration of some chemical compounds and the relative abundances of
364 bacterial genera or fungal species. For examples, mannitol-arabitol and *Alternaria* sp.
365 BMP_2012 (r=0.73 and pvalue=4.8×10^{-9}) and mannitol-arabitol and *Pseudotaeniolina*
366 *globosa* (r=-0.66 and pvalue=5.6×10^{-7}) (**Table S7**).

367

368 ***Weather characteristics: local meteorology and air mass geographical origin***

Temperature, wind speed and UV radiation (weekly averages) varied over the year (pvalue<0.05), conversely to wind direction and relative humidity. The mean weekly temperature varied between -5.5°C and 17.6°C (**Fig. S3**) and was significantly correlated to the season (pvalue=1.4×10^{-11} – **Fig. S10**). Wind speed varied between 2.8 and 13.5 m/s on average, and this was significantly higher in winter compared to summer and spring (pvalue=2.1×10^{-3}, **Fig. S10**), and significantly more variable in winter compared to the other seasons (pvalue=5.4×10^{-4}). Wind speed and direction were positively correlated (r=0.44, pvalue=0.001) with stronger winds coming from West. Nevertheless, the mean wind direction was not significantly different between seasons (pvalue=0.11) and the air mass origins were only partially correlated to the seasons (16% and 14% of the variance explained, pvalue=0.013). The wind roses and the backtrajectory density plots for each season are presented in **Fig. S10** and **Fig. S11**. The seasonal weekly variability in wind conditions, temperature and relative humidity are shown in **Table S3**.

Bacterial concentration correlated best with UV radiation (r=0.38, pvalue=$5.4\text{x}10^{-3}$) and fungal concentration correlated best with temperature (r=0.38, pvalue=5.6×10^{-3}) (**Table S8**). A significant and strong correlation was also found between both the bacterial and fungal community structures and the overall meteorology (*i.e.* temperature, relative humidity, wind direction and speed) (r=0.57 pvalue=0.001 and r=0.48 pvalue=0.001). Bacterial richness was strongly correlated with temperature (r=0.52, pvalue=7.7×10^{-5}) while fungal richness best correlated with wind direction (r=0.50, pvalue=4.6×10^{-4}) (**Table S8**).

Discussion

Seasonal variation in airborne microbial community composition due to changes in local landscapes

Previous investigations of the temporal variations of airborne microbial communities have consistently shown a seasonal shift in both cell concentration and community structure[2,9–12]. This was explained mainly by changes in the surrounding landscape condition[10,11,27] (*e.g.*, vegetation in summer, snow cover in winter *etc*.), local meteorology[2,9] and/or the origin of the air masses (*i.e.* changes in the global air circulation)[9]. Our data showed that seasonality was correlated to the temporal distribution of airborne microbial community structure at puy de Dôme. With these results, we demonstrated the importance of local regional sources (*i.e.* within 50 km) even at relatively elevated sites such as puy de Dôme. Puy de Dôme is mainly surrounded by croplands and/or natural vegetation (> 80% of the surface within a 50 km perimeter based on MODIS satellite images; **Fig. 1**) that undergo strong changes over the year at such latitudes (see puy de Dôme monthly satellite images in **Fig. S1** for an overview). These changes are partly associated with crops (mainly wheat and grain maize) and vegetation that cycle through their different phases on an annual basis. Changes in landscape characteristics are themselves under direct influence of climatic conditions, including precipitation rate, temperature and sunlight exposure. This consequently has a critical influence on the surface microbial communities[28,29]. Over the year, different microorganisms with different trophic modes were likely aerosolized (**Fig. 3**). Fungal phytopathogens (like *Ustilago hordei*) and leaf-associated fungi (like *Naevala minutissima*) increased in relative abundance during the spring and summer periods when the crop plants grew and trees were green; while saprotrophs (like *Cladophialora protea*) increased in relative abundance during the autumn and winter periods after crop harvesting and when dead and decomposing biological material covered terrestrial surfaces. Similar to fungi, soil-associated bacterial taxa (like *Hymenobacter*) were observed in higher relative abundance in autumn and winter and bacterial phytopathogens and leaf-associated bacteria (like *Sphingomonas*) were observed in higher relative abundance in spring and summer. The three general trends (*i.e.* an increase of

specific taxa in autumn/winter; an increase of other taxa in summer/spring; stable or randomly variable microbial taxa over the year – **Fig. 4**) might have driven the distribution of the samples based on both the airborne bacterial and fungal community structures in two major clusters (*i.e.* an autumn/winter cluster versus a spring/summer cluster observed in **Fig. 2**). In addition, the period during which we observed an increase in the relative abundance of a winter or summer-associated microbial taxon varied in length and might have been specific to the life strategy of the given taxon. Microbial taxa whose relative abundance remained stable or varied randomly over the year might partly belong to taxa associated to decomposing matter (the trophic mode of all the fungal taxa present in this group was saprotroph) that is present the whole year. Airborne fungal community structure showed a stronger seasonal variation than bacterial community structure did, likely related to a higher number of fungal taxa showing a seasonal pattern as compared to bacterial taxa (40/50 and 31/50 for fungi and bacteria, respectively). The stronger seasonal shift observed in airborne fungi might be explained by a greater influence of vegetation on fungi as compared to bacteria[30].

Role of local meteorology in the intraseasonal variability of airborne microbial community composition

Local meteorology might also play a role in the temporal distribution of airborne microbial communities at puy de Dôme especially on their intraseasonal variability. In a previous study considering numerous sampling sites[1], we highlighted the importance of local meteorology (especially wind speed, wind direction and temperature variability over time) on the variability of airborne microbial communities when the site was surrounded by a variety of landscapes. Puy de Dôme is characterized by strong wind speeds and highly variable meteorological conditions partly explained by its central position and its high elevation within the Chaîne des Puys mountain range (+1465 m altitude above sea level and up to 500 m above

surrounding landscapes). The wind direction changed rapidly both within and between the weeks. The relative humidity and temperature also showed a high variability within and between the weeks within the same season (**Table S3**). While the correlation between meteorological parameters and airborne microbial communities at puy de Dôme is mainly explained by seasonality, local meteorological parameters might have also affected airborne microbial structures by influencing the aerosolization process as discussed in Tignat-Perrier et al. (2019)[1]. For example, specific temperatures might activate the sporulation of specific fungi[31]. The high correlation observed between temperature and airborne bacterial richness might be explained by the increased turbulence in air, a higher microbial diversity in the sources (*i.e.* surrounding landscapes)[32–35] as well as a drier surface favoring cell and biofilm detachment. Wind parameters were the meteorological parameters that best correlated to airborne fungal richness. Stronger winds are obviously more likely to aerosolize particles from surfaces.

Minor contribution of distant sources in the temporal variation of airborne microbial communities

Weekly averages of wind direction and origin of the air masses did not drastically change throughout the seasons and were highly and randomly variable over the year (**Fig. S10** and **S11**). We did not observe correlations between airborne microbial community structure and the origin of the air masses. In winter, during which free troposphere air masses, and thus potentially long-range transport, have a larger influence[36–38], the variability in the bacterial community structure was not the highest. Marine air masses have been shown to prevail (72%) during winter at puy de Dôme[38]. One sample showed an especially strong marine signature in terms of chemistry (February 2nd, 2017). However, this sample has similar proportion of marine bacterial genera (*Corialomargarita*, *Rubritalea, Aquimarina*) as other

samples. Whenever present, the identified specific marine bacterial genera were very rare (they were represented by only 2 or 3 sequences over > 20000 sequences per sample). Unlike previous suggestions for cloud water-associated microorganisms at this site, microbial communities in the dry phase did not seem to mainly originate from oceanic sources[27]. Uetake et al. (2019)[2] investigated airborne (not cloud-associated) microbial communities in Tokyo (Japan) over a year and also highlighted the absence of oceanic related bacteria (*i.e.* SAR group, *Oceanospirillales*) that would have suggested transport of airborne microbial cells from the Pacific Ocean to Tokyo.

We also observed a seasonal change in the particulate matter chemistry (PM10 chemistry) (**Fig. S7**). At puy de Dôme, changes in PM10 chemistry throughout the seasons were correlated to changes in air mass origins (local and distant) and changes in the vertical stratification of the atmospheric layers (such as the increase of the height of the mixed layer in summer)[36,37]. We observed specific and strong correlations between some chemical species and microbial taxa (**Table S7**) and this could explain the overall correlation between the overall PM10 chemistry and airborne microbial structure. In particular, we observed correlations between specific microbial taxa and polyols. The concentration of atmospheric polyols might be due to the presence of airborne green plant debris as well as specific microbial taxa and especially fungal taxa which produce polyols[39–42]. Our sampling strategy (one-week sampling) might not have been adapted to identify microbial long-range transport events that, if they occurred, might have been greatly diluted by the local sources. Investigations on the temporal variability of airborne microbial communities that concluded the significant contribution of distant sources in the composition of airborne microbial communities[9,13] had either a different sampling strategy than ours (*i.e.* shorter sampling duration such as 24 h[9]) or did not sample microorganisms of the dry phase of the troposphere[13].

Conclusion

We investigated changes in airborne microbial community concentration and structure at the elevated continental site puy de Dôme in the Massif Central of France (+1465 m altitude above sea level) as a function of the local meteorology and particulate matter chemistry. We showed that puy de Dôme airborne microbial community structure likely shifted throughout the year in relation to the seasonal changes in surface conditions of the surrounding landscape of the mountain that was characterized mainly by croplands and natural vegetation. The microbial taxa that drove the seasonal distribution of airborne microbial communities showed different trends throughout the seasons depending on their trophic mode. Crop-associated microorganisms and especially crop pathogens were in higher relative abundance in spring/summer while soil-associated microorganisms and dead material-associated microorganisms were found in higher relative abundance in autumn/winter. Changes in the vertical stratification of the atmospheric layers throughout the seasons (such as the increase of the height of the mixed layer in summer) might also play a role in the seasonal shift of puy de Dôme airborne microbial communities. Within the different seasons, the temporal variability observed in the composition of airborne microbial communities was likely associated to the variable and windy meteorological conditions observed in puy de Dôme.

Acknowledgements

This program was funded by ANR-15-CE01-0002–INHALE, Région Auvergne-Rhône Alpes and CAMPUS France. The chemical analyses were performed at the IGE AirOSol platform. We thank L.Pouilloux for computing assistance and maintenance of the Newton supercalculator.

Competing interests

The authors declare no competing interests.

Data availability

Sequences reported in this paper have been deposited in ftp://ftp-adn.ec-lyon.fr/aerobiology_Puy-de-Dome_amplicon_INHALE/. A file has been attached explaining the correspondence between file names and samples.

Author contribution

AD, PA, CL and TMV designed the experiment. PA, AT, MJ and KS conducted the sampling field campaign. RTP did the molecular biology, bioinformatics and statistical analyses. RTP, AD, CL, TMV analyzed the results. RTP, TM, AD, PA and CL wrote the manuscript. All authors reviewed the manuscript.

References

1. Tignat-Perrier, R. *et al.* Global airborne microbial communities controlled by surrounding landscapes and wind conditions. *Sci Rep* **9**, 1–11 (2019).
2. Uetake, J. *et al.* Seasonal changes of airborne bacterial communities over Tokyo and influence of local meteorology. *bioRxiv* 542001 (2019) doi:10.1101/542001.
3. Amato, P. *et al.* A fate for organic acids, formaldehyde and methanol in cloud water: their biotransformation by micro-organisms. *Atmospheric Chemistry and Physics* **7**, 4159–4169 (2007).
4. Vaïtilingom, M. *et al.* Contribution of Microbial Activity to Carbon Chemistry in Clouds. *Appl Environ Microbiol* **76**, 23–29 (2010).
5. Ariya, P. A., Nepotchatykh, O., Ignatova, O. & Amyot, M. Microbiological degradation of atmospheric organic compounds. *Geophysical Research Letters* **29**, 34-1-34–4 (2002).

6. Pöschl, U. *et al.* Rainforest Aerosols as Biogenic Nuclei of Clouds and Precipitation in the Amazon. *Science* **329**, 1513–1516 (2010).
7. Brown, J. K. M. & Hovmøller, M. S. Aerial dispersal of pathogens on the global and continental scales and its impact on plant disease. *Science* **297**, 537–541 (2002).
8. Mhuireach, G. Á., Betancourt-Román, C. M., Green, J. L. & Johnson, B. R. Spatiotemporal Controls on the Urban Aerobiome. *Front. Ecol. Evol.* **7**, (2019).
9. Innocente, E. *et al.* Influence of seasonality, air mass origin and particulate matter chemical composition on airborne bacterial community structure in the Po Valley, Italy. *Sci. Total Environ.* **593–594**, 677–687 (2017).
10. Bowers, R. M., McCubbin, I. B., Hallar, A. G. & Fierer, N. Seasonal variability in airborne bacterial communities at a high-elevation site. *Atmospheric Environment* **50**, 41–49 (2012).
11. Bowers, R. M. *et al.* Seasonal variability in bacterial and fungal diversity of the near-surface atmosphere. *Environ. Sci. Technol.* **47**, 12097–12106 (2013).
12. Franzetti, A., Gandolfi, I., Gaspari, E., Ambrosini, R. & Bestetti, G. Seasonal variability of bacteria in fine and coarse urban air particulate matter. *Appl. Microbiol. Biotechnol.* **90**, 745–753 (2011).
13. Cáliz, J., Triadó-Margarit, X., Camarero, L. & Casamayor, E. O. A long-term survey unveils strong seasonal patterns in the airborne microbiome coupled to general and regional atmospheric circulations. *Proc. Natl. Acad. Sci. U.S.A.* **115**, 12229–12234 (2018).
14. Amato, P. *et al.* Metatranscriptomic exploration of microbial functioning in clouds. *Sci Rep* **9**, 1–12 (2019).
15. Amato, P. *et al.* Active microorganisms thrive among extremely diverse communities in cloud water. *PLOS ONE* **12**, e0182869 (2017).
16. Amato, P. *et al.* Survival and ice nucleation activity of bacteria as aerosols in a cloud simulation chamber. *Atmospheric Chemistry and Physics* **15**, 6455–6465 (2015).
17. Vaïtilingom, M. *et al.* Potential impact of microbial activity on the oxidant capacity and organic carbon budget in clouds. *PNAS* **110**, 559–564 (2013).

18. Dommergue, A. *et al.* Methods to investigate the global atmospheric microbiome. *Front. Microbiol.* **10**, (2019).
19. Masella, A. P., Bartram, A. K., Truszkowski, J. M., Brown, D. G. & Neufeld, J. D. PANDAseq: paired-end assembler for illumina sequences. *BMC Bioinformatics* **13**, 31 (2012).
20. Wang, Q., Garrity, G. M., Tiedje, J. M. & Cole, J. R. Naive Bayesian Classifier for Rapid Assignment of rRNA Sequences into the New Bacterial Taxonomy. *Applied and Environmental Microbiology* **73**, 5261–5267 (2007).
21. Deshpande, V. *et al.* Fungal identification using a Bayesian classifier and the Warcup training set of internal transcribed spacer sequences. *Mycologia* **108**, 1–5 (2016).
22. Nguyen, N. H. *et al.* FUNGuild: An open annotation tool for parsing fungal community datasets by ecological guild. *Fungal Ecology* **20**, 241–248 (2016).
23. Draxler, R. R. & Hess, G. D. An Overview of the HYSPLIT_4 Modelling System for Trajectories, Dispersion, and Deposition. 25.
24. Carslaw, D. Tools for the Analysis of Air Pollution Data. (2019).
25. Dray, S., Dufour, A.-B. & Thioulouse, J. Analysis of Ecological Data: Exploratory and Euclidean Methodsin Environmental Science. (2018).
26. Harrell, F. E. & Dupont, C. Harrell Miscellaneous - Package 'Hmisc'. (2019).
27. Amato, P. *et al.* An important oceanic source of micro-organisms for cloud water at the Puy de Dôme (France). *Atmospheric Environment* **41**, 8253–8263 (2007).
28. Zhang, Q. *et al.* Alterations in soil microbial community composition and biomass following agricultural land use change. *Scientific Reports* **6**, 36587 (2016).
29. Constancias, F. *et al.* Mapping and determinism of soil microbial community distribution across an agricultural landscape. *Microbiologyopen* **4**, 505–517 (2015).
30. Sun, S., Li, S., Avera, B. N., Strahm, B. D. & Badgley, B. D. Soil Bacterial and Fungal Communities Show Distinct Recovery Patterns during Forest Ecosystem Restoration. *Appl Environ Microbiol* **83**, (2017).
31. Pickersgill, D. A. *et al.* Lifestyle dependent occurrence of airborne fungi. *Biogeosciences Discussions* 1–20 (2017) doi:https://doi.org/10.5194/bg-2017-452.

32. Dennis, P. G., Newsham, K. K., Rushton, S. P., O'Donnell, A. G. & Hopkins, D. W. Soil bacterial diversity is positively associated with air temperature in the maritime Antarctic. *Sci Rep* **9**, 1–11 (2019).
33. Zhou, J. *et al.* Temperature mediates continental-scale diversity of microbes in forest soils. *Nature Communications* **7**, 12083 (2016).
34. Nottingham, A. T. *et al.* Microbes follow Humboldt: temperature drives plant and soil microbial diversity patterns from the Amazon to the Andes. *Ecology* **99**, 2455–2466 (2018).
35. Tittensor, D. P. *et al.* Global patterns and predictors of marine biodiversity across taxa. *Nature* **466**, 1098–1101 (2010).
36. Venzac, H., Sellegri, K., Villani, P., Picard, D. & Laj, P. Seasonal variation of aerosol size distributions in the free troposphere and residual layer at the puy de Dôme station, France. *Atmospheric Chemistry and Physics* **9**, 1465–1478 (2009).
37. Bourcier, L., Sellegri, K., Chausse, P., M. Pichon, J. & Laj, P. Seasonal variation of water-soluble inorganic components in aerosol size-segregated at the puy de Dôme station (1,465 m a.s.l.), France. *Journal of Atmospheric Chemistry* **69**, (2012).
38. Freney, E. J. *et al.* Seasonal variations in aerosol particle composition at the puy-de-Dôme research station in France. *Atmospheric Chemistry and Physics* **11**, 13047–13059 (2011).
39. Medeiros, P. M., Conte, M. H., Weber, J. C. & Simoneit, B. R. T. Sugars as source indicators of biogenic organic carbon in aerosols collected above the Howland Experimental Forest, Maine. *Atmospheric Environment* **40**, 1694–1705 (2006).
40. Ruijter, G. J. G. *et al.* Mannitol Is Required for Stress Tolerance in Aspergillus niger Conidiospores. *Eukaryot Cell* **2**, 690–698 (2003).
41. Solomon, P. S., Waters, O. D. C. & Oliver, R. P. Decoding the mannitol enigma in filamentous fungi. *Trends Microbiol.* **15**, 257–262 (2007).
42. Lewis, D. H. & Smith, D. C. Sugar alcohols (polyols) in fungi and green plants. *New Phytologist* **66**, 143–184 (1967).

626